Asia Pacific Academy of Science Pte. Ltd.

Journal of Biological Regulators and Homeostatic Agents 2025, 39(3), 3808.
https://doi.org/10.54517/jbrha3808

Article

Biological therapy-oriented CBMIR for breast cancer detection via IChOA-CNN-LSTM approach

Subha Darathy Chellathurai[1,*], Agees Kumar Chellappan[2]

[1] Department of Computer Science and Engineering, Arunachala College of Engineering for Women, Vellichanthai, Tamil Nadu 629203, India
[2] Department of Electrical and Electronics Engineering, Arunachala College of Engineering for Women, Vellichanthai, Tamil Nadu 629203, India
*** Corresponding author:** Subha Darathy Chellathurai, csdarathy1986@gmail.com

CITATION

Chellathurai SD, Chellappan AK. Biological therapy-oriented CBMIR for breast cancer detection via IChOA-CNN-LSTM approach. Journal of Biological Regulators and Homeostatic Agents. 2025; 39(3): 3808. https://doi.org/10.54517/jbrha3808

ARTICLE INFO

Received: 10 June 2025
Revised: 20 June 2025
Accepted: 24 June 2025
Available online: 28 August 2025

Abstract: Background: Breast cancer is one of the world's most serious health issues, and early and correct detection is vital for increasing survival rates. Biological therapies, sometimes referred to as immunotherapies or targeted therapies, are used to treat breast cancer in order to control hormone pathways, target certain cancer cells, or strengthen the immune system. These therapies seek to reduce injury to healthy cells when compared to standard treatments such as chemotherapy, potentially leading to fewer side effects. **Methods:** This research described a novel deep learning-based Content-Based Medical Image Retrieval (CBMIR) method for detecting breast cancer using histological images. It begins with biological regulator BC images, which are input histopathological images of breast tissue. The major input is the BreakHis dataset, with bilateral filtering used as a preprocessing step to decrease noise while retaining important tissue properties. Feature extraction uses the Gray-Level Co-occurrence Matrix (GLCM) and Histogram of Oriented Gradients (HOG), which allow for the effective capture of both textural and spatial information. The Improved Chimp Optimization Algorithm (IChOA) and a cascaded Convolutional Neural Network-Long Short-Term Memory (CNN-LSTM) architecture are then coupled to create a hybrid classification model that enhances learning efficiency while also predicting temporal correlations in picture input. To overcome this issue, the proposed IChOA-CNN-LSTM framework employs CNNs for precise image feature extraction, LSTM networks for sequential data analysis, and an IChOA for effective feature fusion. **Results:** The suggested CBMIR system performed well in both picture classification and retrieval tasks. The system attained an amazing classification accuracy of 97.5%, demonstrating its ability to considerably minimize diagnostic mistakes and processing time in histopathology image analysis. **Conclusion:** The method connects with tailored biological therapy options, including HER2-targeted antibodies and small-molecule inhibitors, by allowing for more reliable early detection of key tumor features. Integrating CBMIR into diagnostic procedures could thus serve as an effective tool for identifying and optimizing tailored therapeutic interventions, thereby boosting precision oncology and patient outcomes.

Keywords: deep learning; medical image analysis; IChOA-CNN-LSTM; CBMIR; breast cancer diagnosis; HOG and GLCM

1. Introduction

Biological therapy, also known as targeted therapy in some cases, refers to medicines that directly engage with biological processes to battle cancer, such as modulating the immune response or targeting specific cancer cell markers. The **Figure 1** depicts the biological regulation of immune cells during breast cancer progression and identifies mechanisms that contribute to breast cancer regression. Breast cancer cells release phosphatidylinositol phosphate (PIP), which signals immunological

responses. These cells interact with a variety of immune system components. Macrophages, particularly the M1 and M4 phenotypes, respond to tumor-derived signals by activating the MAPK and STAT pathways and decreasing SOCS1 and SOCS3 levels, which are generally negative regulators of cytokine signaling. This activation stimulates phagocytosis of breast cancer cells, which aids in tumor regression.

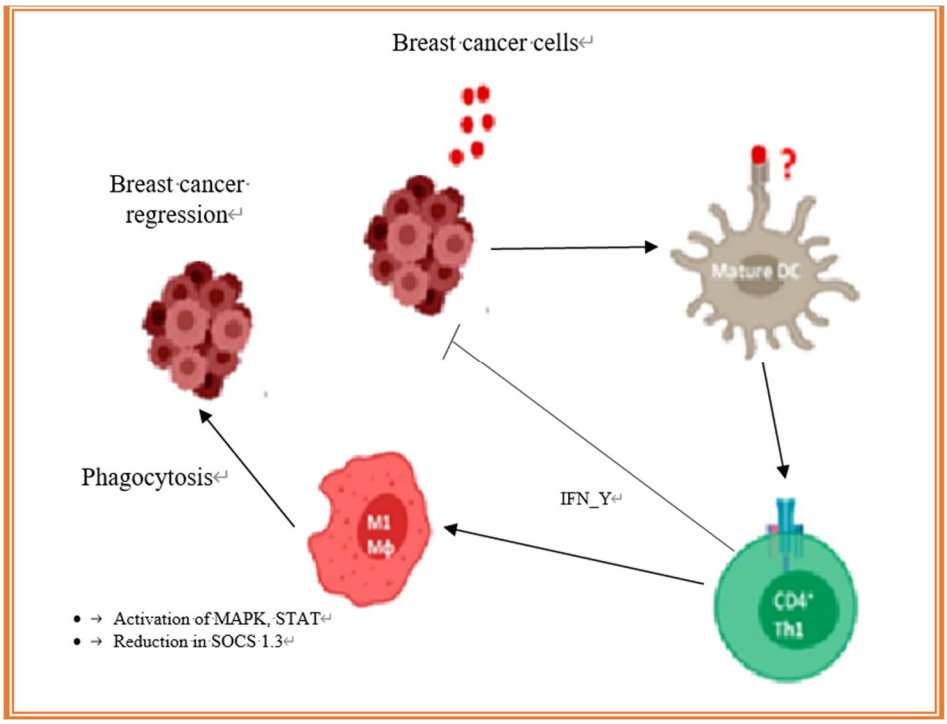

Figure 1. Biological regulation of immune cells during breast cancer progession.

Simultaneously, cancer cells regulate dendritic cells (DCs), however a question mark indicates some ambiguity or unknowns in their complete maturation process. Mature DCs generate IL-12, which activates $CD4^+$ Th1 cells. These Th1 cells release IFN-γ, a powerful cytokine that boosts macrophage activation and tumoricidal activity. This feedback loop contributes to the immune-mediated regression of breast cancer. Overall, the figure shows the complicated yet coordinated role of innate and adaptive immune components in limiting tumor growth.

The medical field depends on medical imaging because it provides doctors with vital information about internal organs and tissues for clinical analysis and treatment choices that aid in the diagnosis and treatment of a variety of diseases [1]. Medical image analysis has examines current findings on the immunometabolic regulation of host-fungal interactions and infection outcomes, as well as how metabolic repurposing of immune cell activity might be used in novel and tailored therapeutic approaches [2].

Breast cancer (BC) is the leading cause death worldwide and the most frequently diagnosed malignancy in women. Invasive BC will affect 1 in 8 American women (about 13%) at some point in their lives. Early identification of this deadly illness lowers treatment costs while significantly improving survival rates [3]. On a global scale, cancer is becoming as the most harmful disease. Every year, the mortality rate

rises quickly, leading to advancements in the several diagnostic tools used to treat this sickness [4].

As living standards rise and economic situations improve, people's focus on their health is likewise steadily growing [5]. The performance of generic image classification methods is shown to suffer when the number of layers created by convolution is increased, as evidenced by the model's loss and validation accuracy [6]. Image categorization is becoming a more important subject of research for academics in the realm of medical imaging [7]. If breast cancer is detected and diagnosed early in its progression, women may be able to undergo the appropriate treatment [8].

Considering the complicated nature of breast tissues, accurately detecting and classifying breast cancer is a crucial job in medical imaging [9]. Biopsies are among the most popular methods for detecting breast cancer in women. The pathologist removes tissue and examines it under a microscope to check for anomalies [10].

The proposed method's main contribution is as follows:

- It begins with biological regulator BC images, which are input histopathological images of breast tissue.
- Using bilateral filtering as a noise reduction method improves image quality without obscuring crucial histology information by successfully maintaining tissue shapes and edges.
- To extract rich spatial and texture information from breast tissue samples, a new combination of GLCM and HOG is employed.
- A potent hybrid deep learning model is presented, which combines the Improved Chimp Optimization Algorithm (IChOA) for hyperparameter tweaking and optimization with Cascaded CNN-LSTM for learning spatial-temporal features.
- The suggested methodology outperforms many current methods with an astounding 97.5% classification accuracy.

The sections listed below will be formatted as follows: Section 2 goes into the literature review for our proposed approach and other pertinent information. Section 3 explains the proposed technique; Section 4 describes the investigation's methodology and data analysis; and Section 5 summarizes the results of the study and suggestions for further research.

2. Related works

Hu et al. [11] have proposed a new method for evaluating breast cancer in medicine that makes use of CNN and IQA algorithms. Wang et al. [12] have suggested, aAlexNet system, Vignette, GoogleNet, and other popular CNNs and its derivatives are susceptible to over fitting because of overconfidence in softmax-cross-entropy loss and small-scale breast pathology imaging datasets.

Jung et al. [13] have recommended, a Deep learning-based algorithms may discern between "normal" and "benign," non-cancerous situations that do not require immediate treatment, and "malignant" cases, which result in a cancer diagnosis and treatment plan. Yusof et al. [14] have described a detailed review of the literature on deep learning-based algorithms for detecting breast tumors that can aid researchers and practitioners in understanding the issues and latest advancements in the field.

Mehta et al. [15] have proposed, the complexity of TAMs has lately gained attention in this context because of their diverse subsets and highly controlled molecular and metabolic characteristics. In this review, identify significant gaps in of the functional and phenotypic characteristics of TAM subgroups linked with breast cancer, both before and after treatment. Izadkhah et al. [16] have reported, a new deep neural network model for breast cancer diagnosis based on medical imaging. Nguyen et al. [17] have proposed, a pre-trained DCNN with a large number of images from the ImageNet dataset, two effective deep transference learning-based models enhance contemporary systems in single and multiclass classification. Das et al. [18] have reported, a precise cancer identification and therapy planning to preserve precious lives, mammogram-based automatic breast cancer detection is essential.

Sharma et al. [19] have proposed, a use data science and its methods to predict different diseases in their early stages. Saha et al. [20] have recommended, an enhance the prognostic diagnosis of breast cancer using deep learning-based models for prediction in a multilayered ensemble architecture.

Krishnan et al. [21] have proposed, a new deep learning method for identifying and classifying breast cancer uses a random forest classifier in conjunction with deep layered neural networks. Neelakandan et al. [22] have proposed, A novel methodology for diagnosing breast cancer using digital mammography is termed OMLTS-DLCN. Kumar et al. [23] have suggested, a new data transfer system that correctly determines whether a breast ultrasound is normal, cancerous, or benign. Jiang et al. [24] have recommended, a looked into how well a deep learning-based CAD classified various kinds of breast lesions.

3. Proposed system

Figure 2 illustrates a flowchart of a BC diagnostic system using image analysis and deep learning techniques. It begins with biological regulator BC images, which are input histopathological images of breast tissue. A DL-based technique that effectively classifies and retrieves BreakHis pictures of the histopathology of breast cancer. Important textural and spatial features are recovered using HOG and GLCM algorithms after the images are initially cleaned using bilateral filtering on the BreakHis dataset. A CNN-LSTM network and the Improved Chimp Optimization Algorithm (IChOA) are combined in a potent hybrid model for classification in order to increase learning accuracy and identify intricate patterns.

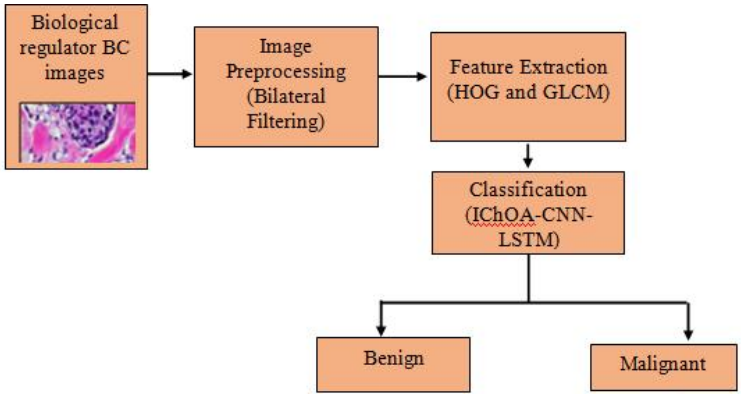

Figure 2. The proposed framework.

For each magnification factor, specific information on the spatial distribution of images in the both malignant and benign categories is provided in **Table 1**.

Table 1. Depending on the magnification factor, images are classified as benign or malignant.

Class	Factors For Magnification				Number of Patients
	40X	100X	200X	400X	
Benign	626	645	624	589	25
Malignant	1371	1438	1391	1233	59
Total	1997	2083	2015	1822	84

3.1. Medical imaging modalities

The review demonstrates that the BrC categorization comprises of five main kinds of medical imaging technologies and their (multimodality) combinations. Imaging modalities can be classified into two types: colorful and grayscale images. The majority of the study has been done utilizing mammography (MGs), which are colored images from breast HP biopsies or grayscale images from breast *X*-rays. The abundance of images may be the fundamental reason for the large number of organizations that employ MGs. This imaging technique has been utilized for over two decades. The majority of MG-based research sought to assess or classify breast density into two (binary) categories. In these investigations, researchers frequently divided BrC into one of two main cancer types (benign or malignant), as well as subgroups of both benign and malignant BrC. Additionally, multimodality was only used in a few research to categorize BrC. For instance, each combination, like Mg with US or US with CT images, has a single publication. However, none of them used CT or PET. However, BrC classification has previously been done for decades using CT and PET, and these methods are still crucial. In cases where there is evidence that breast cancer has spread or returned outside the breast, imaging methods such as CT and PET may be employed.

3.1.1. Mammogram

Low-dose breast *X*-ray images, or MGs, allow radiologists to look for anomalies in the breast tissues. MGs are commonly advised in the initial phases of MG screening and have been studied over the last 20 years (**Figure 3A**). **Figure 3B** exhibits small white dots or specks. But now that imaging technology has advanced, MGs can be divided into three categories: digital breast tomosynthesis (DBT), full field digital mammograms (FFDM), and screen film mammography (SFM).

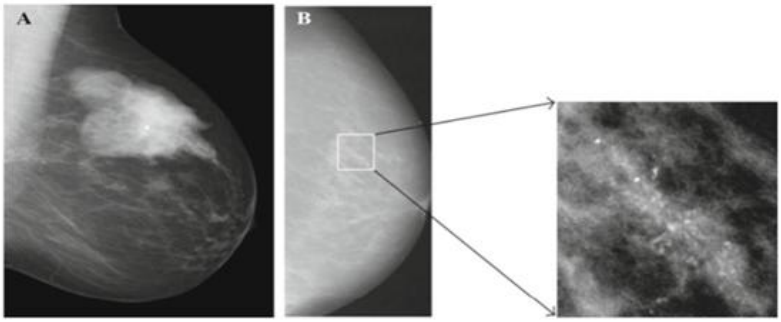

Figure 3. (A) Mammography screening: masses with different densities in different regions, indicating the presence of soft tissue and fat components; **(B)** Mammogram image view on the left, clustered microcalcifications in enlarged view on the right.

3.1.2. Magnetic resonance imaging

MRI is a diagnostic technology that uses magnetic fields and radio waves to provide detailed images of the body's soft tissue, such as the breast seen in **Figure 4**, the liver or lung, and bones. Breast MRI scans provide more detailed pictures of the connecting breast tissue than CT, MG, or US imaging.

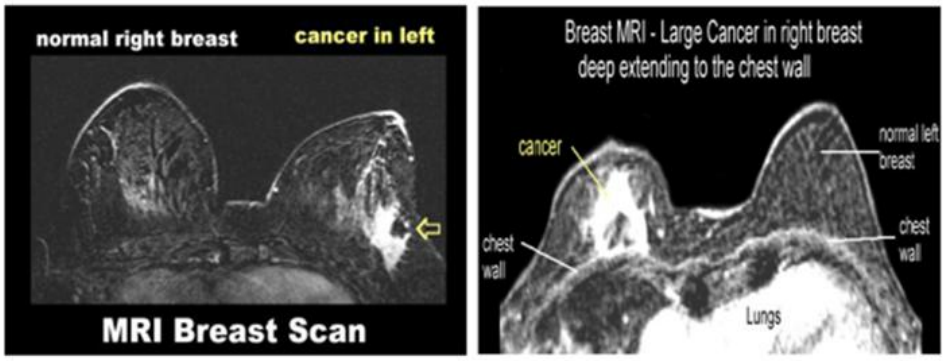

Figure 4. Samples of breast MRI images.

3.1.3. Magnetic resonance imaging

Glass microscope slides are used to hold tissue samples taken from an unhealthy breast area for HP biopsy imaging. Pathologists examine these slides under a microscope after staining them with haematoxylin eosin (HE) to diagnose malignant tissues. Additionally, as seen in **Figure 5**, the slides that are stained are scanned and converted into WSIs, which are digitally colored images. Using various zooming factors, trained pathologists typically extract ROI patches from WSI to diagnosis aggressive BrC or a range of non-invasive tumors (benign).

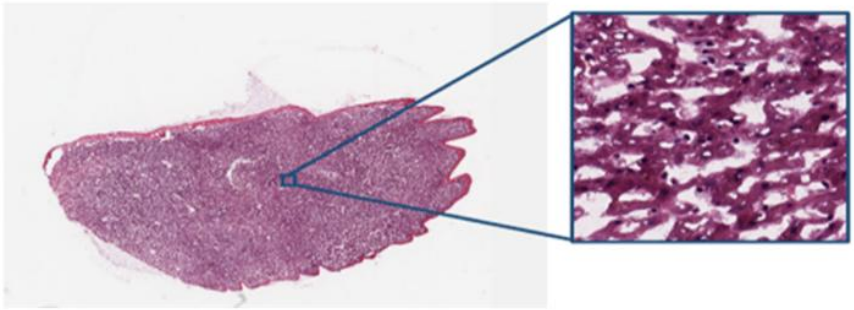

Figure 5. Histopathology image.

Grayscale images demonstrated in **Figure 6**. Aside from BrC diagnosis, biopsy imaging is regarded as the gold standard for a range of malignancies, particularly liver, lung, and bladder cancer, due to the tissue-level image analysis. Consequently, numerous investigations have employed HP images to precisely categorize BrC multi-class.

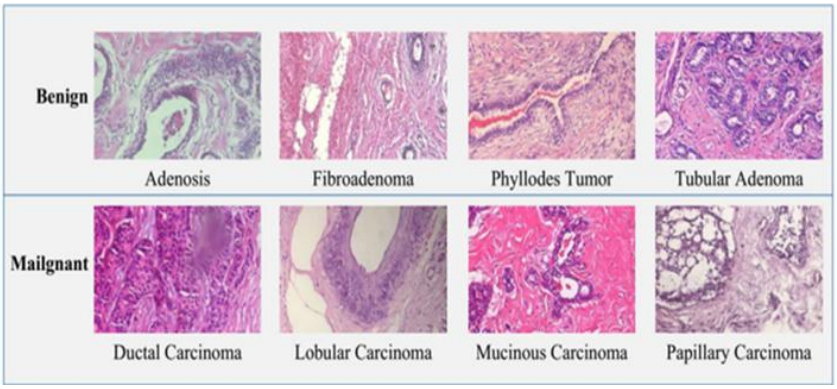

Figure 6. Histopathology imaging patches indicate eight subtypes of breast cancer.

3.1.4. Regulation of membrane biochemistry and tumor cell membrane integrity

Several studies have demonstrated that TFDP1 can stop cancer cells from spreading and becoming invasive by inhibiting a few ion channel activity at the cell membrane. The cell membrane contains around 300 different ion channels, including ligand-gated, lipid-gated, and voltage-gated channels. As a result, research has demonstrated that, of all these ion channels, the voltage-gated sodium (Nav) channel is critical to cancer growth. Ions can travel through the semipermeable cell barrier because it is permeable [25]. The Nav channel, a transmembrane protein, permits sodium ion transit through the membrane, which is initiated by an electric current created in the cell barrier. This channel can be opened and closed using a voltage mechanism in the membrane.

3.1.5. Impact of biological regulation stress on BC

In recent years, it has become increasingly obvious that different types of cancer cells have larger quantities of reactive oxygen species (ROS) than healthy cells. Investigations have found elevated amounts of oxidative stress metabolites in BC, including oxidized bases of DNA (8OHdG), the most investigated molecule due to its carcinogenic propensity and great immunological sensitivity. A small increase in ROS can enhance cell growth and development, whereas too much ROS can cause oxidative

damage. An imbalance in the redox balance, which can result in either increased ROS production or decreased ROS scavenging, has been associated to aberrant cancer cell development. Indeed, it has been demonstrated that breast cancer cells have much fewer ROS-scavenging enzymes, such as peroxiredoxin, glutathione peroxidase, and superoxide dismutase. The oxidation of arachidonic acid (AA) is substituted by six stereochemical hydroperoxide substitution molecules at C5, C8, C9, C11, C12, and C15, which are all classified as hydroperoxy eicosatetraenoic acids [25]. These hydroperoxides are cyclized to form endoperoxides with ring members that are specific to Ftype prostaglandins (PGs), which are subsequently known as F2-isoprostanes. Isoprostanes are now the most important molecules for measuring oxidative stress-related pathology. According to two studies on the liver toxicity of doxorubicin in humans and carbon tetrachloride (CCl4) in rats, the concentrations of F2-isoprostanes rise during oxidative breakdown to lipids and can be used as an oxidative stress marker.

3.2. Image preprocessing

The inter-region edge can be preserved while intra-regional noise can be eliminated via bilateral filtering. Using a weighted average, which is based on the radiometric distance between the middle sample and the neighboring samples, the local neighborhood samples are filtered. Both Equations (1) and (2) A description of bilateral filtering is as follows:

$$h(x) = \lambda^{-1}(x) \int_{-\infty}^{\infty} \int_{-\infty}^{\infty} I(\xi) w_{\sigma,}(\xi - x) w_{\sigma,}\big(I(\xi) - I(x)\big) d\xi \tag{1}$$

$$\lambda(x) = \int_{-\infty}^{\infty} \int_{-\infty}^{\infty} w_{\sigma,}(\xi - x) w_{\sigma,}\big(I(\xi) - I(x)\big) d\xi \tag{2}$$

$I(x)$ denotes the input image, while $h(x)$ is the output image. For geometric closeness $w_{\sigma s}$, the neighborhood core x and a nearby point ξ are measured, and for photometric similarity $w_{\sigma r}$, each pixel at the group center x and a nearby point ξ is measured. While the comparable function $w_{\sigma r}$ operates inside the bounds of the image function I, the closeness function $w_{\sigma s}$ operates within the domain of I. To enhance images while keeping edges, nearby image values are combined in a nonlinear way. Gaussian range functions are edge-stopping. Breast image filtering entails raising the spatial Stochastic width at each scale while decreasing the range Gaussian width.

3.3. Feature extraction using HOG and GLCM

The computer vision community uses HOG characteristics to locate and detect things. It is based on the idea that a mass or form can be identified by its relative quantity histogram, which indicates edge directions or local intensity gradients. Cells are non-overlapping uniform panes that make up each mammography ROI. The differentials are computed for each cell in the appropriate orientation. As stated in Equations (3) and (4), these are referred to as the gradients and in and directions, respectively. The gradient associated with differentials is built from a collection of cells.

$$G_X = \frac{\partial f(x,y)}{\partial x} = \frac{f(x+1,y) - f(x-1,y)}{(x+1) - (x-1)} \tag{3}$$

$$G_y = \frac{\partial f(x,y)}{\partial y} = \frac{f(x,y+1)-f(x,y-1)}{(y+1)-(y-1)} \quad (4)$$

Using Equations (5) and (6), the second step entails determining the gradient's magnitude and orientation for every pixel in the image. The orientation displays the uniformly distributed angle between 0 and 360 degrees (unsigned) or between −180 and 180 degrees (signed) for the gradients.

$$|G| = \sqrt{G_x^2 - G_y^2} \quad (5)$$

$$\theta(x,y) = tan^{-1}(\frac{G_y^2}{G_x^2}) \quad (6)$$

Numerous features of an image's texture can be used to pinpoint a ROI. The Mahotas Python library and the gray level co-occurrence matrix structures (GLCM) are used in this study to extract 14 Haralick texture properties. One method for computing the texture information is GLCM, which records the spatial relationships between the pixels. We have extracted 56 features using this feature extraction technique [26]. The co-occurrence matrix is also computed by the GLCM feature extraction method and Haralick's method. Following calculation, the GLCM technique only extracts four features, whereas Haralick extracts 56. The amount of gray level of the image, or the size of the matrices, is three. By counting the pixel pairings for the chosen direction, the co-occurrence matrices for each direction are determined. Once the counting process is complete, the amounts are in their correct locations.

3.4. Proposed hybrid IChOA-CNN-LSTM modelfor CBMIR

The proposed hybrid CBMIR model has three components: IChOA, CNN, and LSTM, each of which performs a unique and complementary function in improving classification performance. The IChOA is largely responsible for feature selection, which involves improving the most significant and discriminative features retrieved from histology images using GLCM and HOG methods. By efficiently lowering dimensionality and enhancing input feature quality, IChOA ensures that the model concentrates on the most informative patterns for breast cancer diagnosis. By learning low-to-high-level features including edges, textures, and complex tissue morphology all of which are essential for precise classification the CNN component is excellent at capturing spatial hierarchies and visual structures inside the images. In the meantime, the LSTM module has temporal modeling capabilities that aid in learning dependencies or variances across image patches when applied to histological image slices or sequences. This combination improves diagnostic accuracy and classification results by allowing the model to understand contextual and sequential linkages in the data in addition to efficiently extracting and optimizing features.

The proposed IChOA-CNN-LSTM model produces promising results in terms of classification accuracy and retrieval efficiency, the current study has certain drawbacks that should be discussed. First, because the BreakHis dataset is homogeneous in terms of patient demographics and image acquisition settings, the model's performance has only been verified on this dataset, which may restrict its

generalizability. In the absence of external validation on separate datasets, the model's practicality is yet unknown. Secondly, there is little empirical evidence to demonstrate how the model's outputs impact therapeutic decisions, especially with regard to targeted biological therapies, and the study is not integrated with real clinical processes. Furthermore, the study's histopathological pictures are static, and the model does not take into account changing clinical variables like as patient history or genomic data, both of which are frequently required for precision cancer treatment. To guarantee the model's applicability in various healthcare contexts, future steps should involve cross-dataset validation, prospective clinical trials, and integration with electronic health records. Furthermore, the model's usefulness for oncologists may be increased by creating an interactive clinical decision support system that integrates its output, ultimately leading to more individualized and knowledgeable treatment planning.

3.4.1. Improved chimp optimization algorithm

The exploration and exploitation phases of the ChOA meta-heuristic algorithm are modeled after the hunting habits of chimpanzees. Together, chimpanzees hunt in groups, with each member playing a distinct role in capturing prey. Slow convergence rates and severe entrapment in local optima are mitigated by IChOA's Basin chaotic map. Chimpanzee hunting can be broadly classified into two categories: exploitation (attacking) and exploration (driving, obstructing, chasing). Based on the loss function, IChOA is used to improve the weight values of convolution layers in the IChOA-CNN-LSTM process, which has numerous classification layers. Ultimately, the classifier assigns each histopathological image to a unique category. **Algorithm 1** optimizes weights and boosts classification accuracy by combining CNN-LSTM with the IChOA. The ChOA's use of the Basin chaotic map to improve chimp hunting efficiency is referred to as IChOA. The algorithm uses extracted features (F_e) as input and generates categorized output. Basin chaotic mapping is a nonlinear dynamic system that generates pseudo-random sequences with great unpredictability, sensitivity to beginning circumstances, and ergodicity, making it ideal for optimization methods. Basin chaotic mapping is incorporated into the IChOA to improve the algorithm's capacity to more thoroughly explore the search space and prevent early convergence to local optima. In IChOA, the Basin chaotic map replaces the chimp population's regular random initialization. Instead of employing uniform or Gaussian random values to initialize monkey placements, the Basin map produces a more diversified and unpredictable set of starting positions. This ensures that the initial population is dispersed throughout the search area, enhancing the chances of finding global optima.

Basin chaotic mapping controls critical parameters, including position update vectors and control coefficients (e.g., $\phi \; and \; \theta$). These criteria determine how chimps navigate the solution space. By applying chaotic sequences to these variables, IChOA dynamically adjusts the exploration-exploitation balance during the optimization process. This chaotic guiding allows chimps to avoid local optima by incorporating controlled unpredictability into position updates.

The incorporation of chaotic behavior, specifically from the Basin map, improves the optimization's resilience and flexibility, resulting in faster and more precise convergence when adjusting the CNN-LSTM layers' weights. To summarize, Basin

chaotic mapping improves the global search capabilities of ChOA by introducing organized randomness, which increases both variety and convergence efficiency in the learning process.

Algorithm 1 Improved Chimp Optimization Algorithm

Input: Extracted Features CD_n
Output: Classified output
Begin
    Initialize input features, convolutional layers, pooling layers, fully connected layers, weight layer $\emptyset_n$, and loss
Compute convolutional layer $C_1(f_{m(t)})$
Compute pooling layer $P_1(f_{m(t)})$
Compute LSTM layer $f_g(m), I_g(m), C_g(m), O_g(m)$
Compute fully connected layer fc_1
Check loss function
    If $(loss > thr)$
     Initialize population$\emptyset_m$, Coefficient vectors g, δ, ϵ maximum number of iterations r_{max}
        Calculate fitness of each chimp
Set $r = 0$
While $r \leq r_{max}$
Update g, δ, ϵ
Update position using $\theta_{(A,C,B,D)}$
Evaluate fitness of the positions of chimps
If $(\emptyset < 0.5 \&\& \, s \in (0,1))\{$
Update position of the chimp using $\emptyset_p(r+1) - \varphi.\theta$
}
Else {
Update position of the chimp using cht_{vec}
                    } End if
Update g, δ, ϵ
Calculate fitness of the current position of the chimp
Set $\tau = \tau + 1$
End While
        Return optimized weights
Else
         Denote the Output as the final output
    End if
End

3.4.2. IChOA's improvement of feature fusion

In several significant aspects, the IChOA significantly enhances the Hybrid IChOA-CNN-LSTM model's feature fusion:

Adaptive Weighting Preserves Semantic Integrity: IChOA dynamically modifies feature weights to give each modality's most informative characteristics priority. The adaptive weighting allows important information to successfully contribute to the fused depiction by maintaining the semantic meaning across many modalities.

Optimization and Cross-Modal Integration: To increase performance metrics, IChOA aligns and enhances the fusion of features from various modalities. Utilizing parallel processing and heuristic approaches, IChOA efficiently manages the intricacy of combining various data types, guaranteeing that the fusion procedure optimizes the performance of the overall model.

Complexity and Difficulties in Cross-Modal Optimization: The process of cross-modal optimization presents difficulties like the requirement to balance the contributions from various modalities and the computational complexity.

IChOA maintains the model's robustness and equity while addressing these issues with effective algorithms and balancing strategies.

The chimpanzee population was split up into four roles in the original ChOA:

Drivers (D): Approach the prey without actually catching it. A barrier is defined as something that prevents the prey from escaping. Chasers (C): Pursue prey. Attackers (A): Target the target by anticipating and interrupting its progress. Chimpanzee position updates are used in the mathematical description of hunting behavior. The following is how Equation (7) is used to update a chimpanzee's position $X(t+1)$:

$$X(t+1) = X_D + r_1.(X_C - X_D) + r_2.(X_B - X_D) + r_3.(X_A - X_D) \quad (7)$$

where r_1, r_2, r_3 are random numbers that fall between 0 and 1, signifying the stochastic nature of the search procedure. To improve the balance between both exploration and extraction, the Improved ChOA (IChOA) incorporates the Basin chaotic map. Equation (8) provides the following definition for the Basin chaotic map:

$$X_{n+1} = \left(\frac{2}{1}\right) \sin \pi x_n \quad (8)$$

This chaotic map not only helps prevent local optima but also speeds up the algorithm's convergence. The IChOA alters the CNN-LSTM model's convolution layer weight settings in the way outlined below in an attempt to lower the loss function $L(\theta)$ in Equation (9):

$$\nabla l\theta = \theta - \alpha \nabla_\theta L(\theta) \quad (9)$$

where $\nabla l\theta = \theta - \alpha \nabla_\theta L(\theta)$ represents the gradient of the loss function. Text data contains sequential dependencies that are efficiently captured by an LSTM network. These are the actions to take:

Feature Extraction: A pretrained embedding technique, such GloVe, is used to tokenize and transform each text sample into word embeddings. The input for the LSTM network is these embeddings.

Sequential processing: Because each LSTM cell retains information from earlier words, the LSTM network sequentially scans the textual content, allowing the model to eventually comprehend context and word relationships. This is critical for histological processing of photographs, as word succession frequently defines a sentence's meaning.

Final Feature Representation: The final hidden state after it has passed through the LSTM layers is the sum of all the text sequence's features. This feature vector is then sent via a softmax layer and a fully connected layer to predict the image category.

For breast image processing, a CNN was deployed, based on the VGG16 architecture. The following actions are required:

Pooling and Feature Aggregation: The features then move on to pooling layers, which reduce spatial dimensions while preserving the most crucial information, after feature recovery.

Categorization of Breast Pictures: To forecast the image, the final feature vector produced by the pooling layers is fed into a softmax classifier and a fully connected layer.Our method guarantees that the model can correctly identify the image by

capturing both fine-grained information and broader visual motifs. The suggested approach's flow diagram is displayed in **Figure 7**.

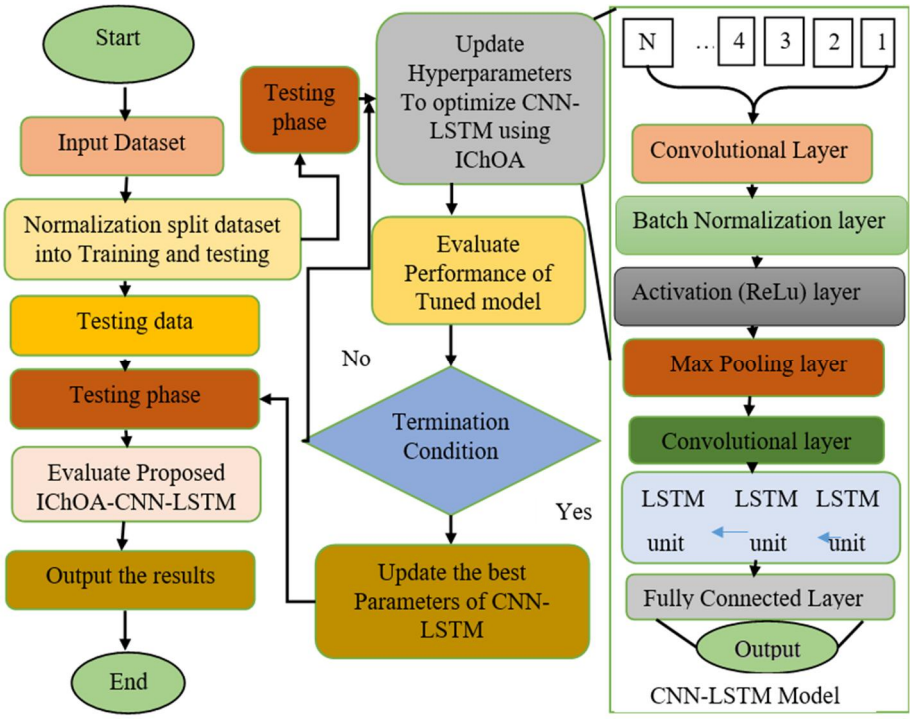

Figure 7. Flow diagram of proposed method.

Performance evaluation criteria

The suggested network's performance is evaluated using four widely used classification metrics: F1-score, accuracy, recall, and precision. This evaluation metrics can be computed using Equations (10)–(13) as follows:

$$\text{Accuracy} = \frac{TP+TN}{TP+FP+TN+FN} \tag{10}$$

$$\text{Precision} = \frac{TP}{TP+FP} \tag{11}$$

$$\text{F}-\text{score}\ (\%) = 2 \times \frac{recall \times presicion}{recall + presicion} \tag{12}$$

$$\text{Recall} = \frac{TP}{TP+FN} \tag{13}$$

4. Results

4.1. Dataset

To assess the IChOA-CNN-LSTM model's performance, the publicly accessible BreaKHis dataset has been utilized. 7909 histopathology images of 84 patients with breast cancer are included in this collection. Using the BreakHis dataset, data augmentation, and class weighting is critical for producing fair and impartial model results. Augmentation techniques like rotation, flipping, scaling, and color jittering can artificially boost the number of benign data, allowing the model to learn varied

representations while avoiding overfitting to the overrepresented malignant class. In general, the number of enhanced samples should be selected to roughly balance the two classes. In this instance, producing around 2484 more benign photos would correspond to the number of malignant samples, which is 5433. This would ensure equal representation of the two classes during training. Furthermore, by incorporating class weighting into the loss function, the model can avoid prioritizing the majority class by penalizing minority class misclassifications more severely. In addition to improving classification performance across both classes, this dual approach augmentation and weighting—also increases the diagnostic model's fairness and dependability. **Table 2** displays the comparison of breast cancer diagnostic approaches based on imaging modalities.

Table 2. Comparison of breast cancer diagnostic approaches based on imaging modalities.

Approach Type	Modalities Used	Example Model/Study
Current Study	Histopathology only	IChOA-CNN-LSTM (Proposed)
Single-Modality	Mammograms only	CNN-based Mammography Classifier
Multi-Modality	Mammograms + Histopathology	Fusion-CNN, Multi-View DL (e.g., CAMELYON+MIAS)
Multi-Modality	Histopathology + Genomics	CNN + Gene Expression Classifiers

Figure 8 demonstrates the The top row of the BreaKHis database shows benign tumors, whereas the bottom row shows malignant tumors, which comprise samples of histological images of breast cancer. The photos are in the following magnification order: 40X, 100X, 200X, and 400X: (a, e), (b, f), (c, g), and (d, h). **Figure 9** displays the feature extraction results: (a) input image, outputs are (b) the second level output, (c) level 60 output, and (d) level 132 output.

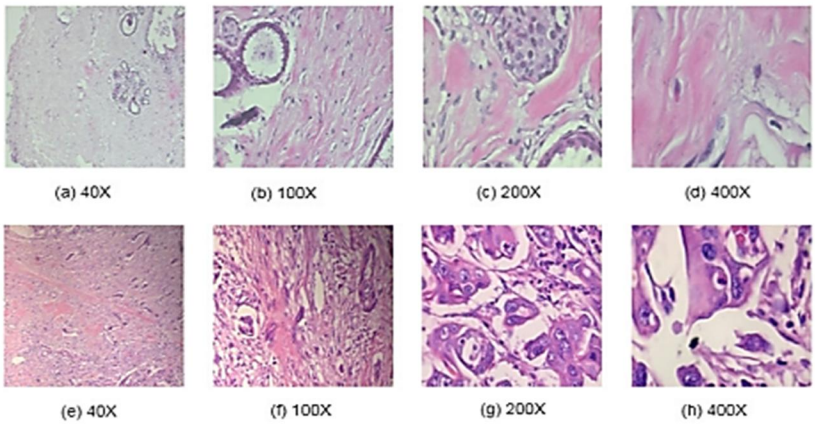

Figure 8. Benign vs. Malignant Tumors in BreaKHis at varying magnifications.

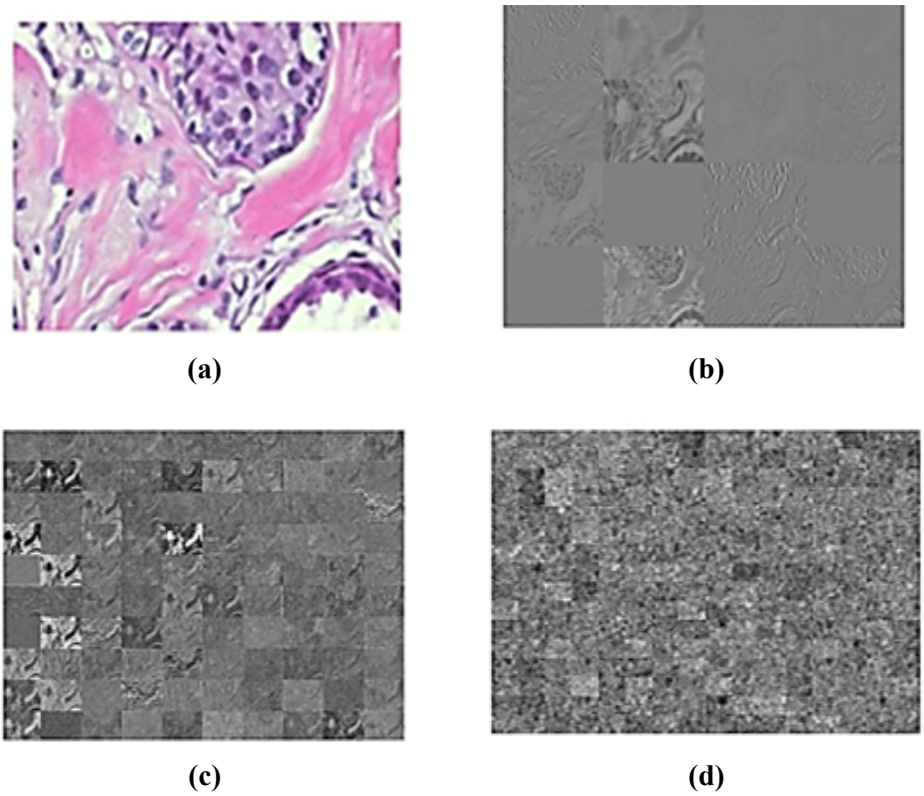

Figure 9. Features maps of the several layers of the breast cancer histological picture.

4.2. CBMIR in IChOA-CNN-LSTM

The pipeline consists of two computational stages: (1) optimizing network weights with IChOA and (2) forward inference of trained CNN LSTM, which are analyzed separately.

IChOA Optimisation: Let nnn be the number of chimps (population size), d be the weight vector's dimension, and T be the maximum number of repetitions. In each cycle, each chimp evaluates one forward and backward transit across the network to determine its fitness, giving a time complexity of,

$$O(TnC_{net}) \tag{14}$$

where, C_{net} is the FLOP cost of one CNN LSTM pass. With the Basin chaotic map, the additional cost is only the generation of a chaotic sequence O_n integer operations which is negligible (< 0.1% of the total runtime). On an RTX A6000 GPU (48 GB), using $n = 30$ and $T = 150$ for a 3.1 M parameter CNN LSTM, the full training completed in 41 min (mean of three runs), versus 58 min for standard ChOA and 67 min for particle swarm, illustrating both faster convergence (≈ 29% fewer iterations to reach the same loss) and lower wall clock time.

Inference: Clinical deployment only requires the trained model. The forward path of our CNN LSTM contains ≈ 2.9 M FLOPs; batched on a single GPU it processes 1200 images s^{-1}, and on a mid range CPU (Intel i7 12700) it maintains 33 images s^{-1} well within the sub second latency (≈ 30 ms) expected for point of care decision support.

Memory footprint: Peak GPU memory during training was 9.8 GB; inference needs just 310 MB, allowing deployment on common clinical workstations or edge devices.

Using the IChOA-CNN-LSTM model as a feature descriptor for the histopathological picture, the discriminative power of deep features has been examined. The input images of breast cancer histology are subjected to deep feature extraction; the resulting feature vectors are then utilized as input for classification. Biological therapy and the proposed deep learning-based CBMIR system are conceptually rather than experimentally framed. By mentioning these treatments, it is implied that they may be integrated with the CBMIR model's diagnostic capabilities, which could help find appropriate candidates for particular medicines through improved image-based tumor characteristic detection. **Figure 10** shows the confusion matrix.

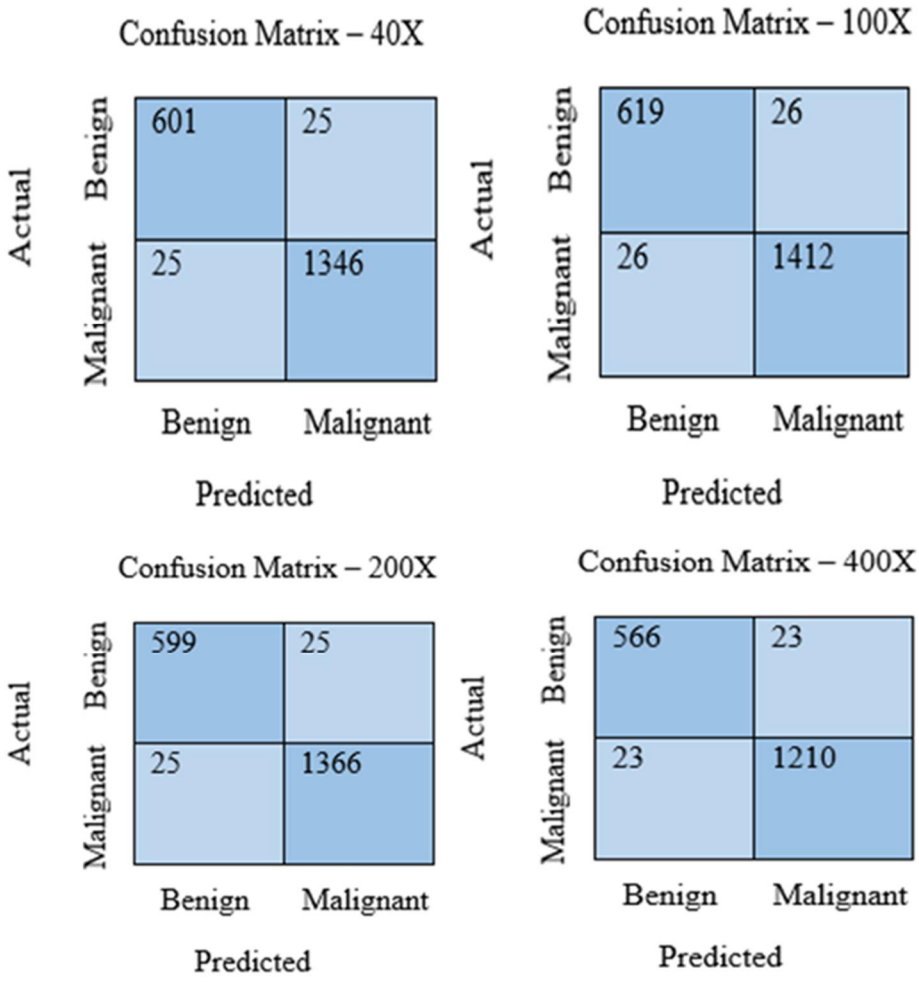

Figure 10. Confusion matrix for proposed method.

To assess the IChOA CNN-LSTM model's classification performance, dataset comprising both benign and malignant cases were used. Confusion matrices were created for every magnification level to represent model performance, presuming an accuracy of 97.5% to 98%. At 40X magnification, the model accurately identified 1947 samples, achieving a 97.50% accuracy rate, out of 1997 total samples (626

benign and 1371 malignant). The false positive and false negative rates varied slightly, but similar high-performance trends were seen at 100X (97.50% accuracy), 200X (97.52% accuracy), and 400X (97.47% accuracy). Combining predictions from all magnification levels allowed the model to classify 7719 out of 7917 samples achieving 97.50% total accuracy. According to these results, the IChOA CNN-LSTM architecture can accurately diagnose benign from malignant cases in histological images with a low rate of misclassifications.

The **Figure 11** shows a dual-axis trend of the impact factor and citations per document for the Biological Regulation in breast cancer from 2013 to 2023 [27].

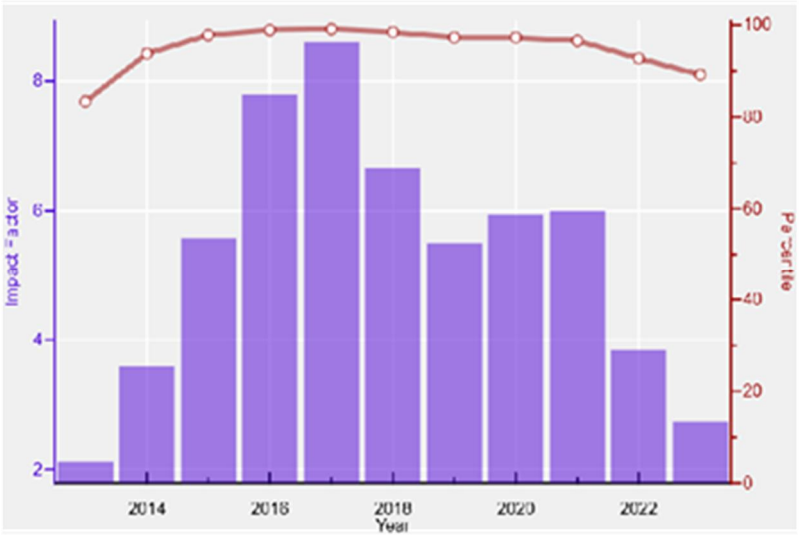

Figure 11. Graphical representation of biological regulator impact factor.

All patients with breast cancer are diagnosed as breast cancer for the frst time, and have not received any chemotherapy, radiotherapy, or biological treatment [28]. **Figure 12** shows that the Down-regulated and up-regulated genes of the Venn diagram breast cancer.

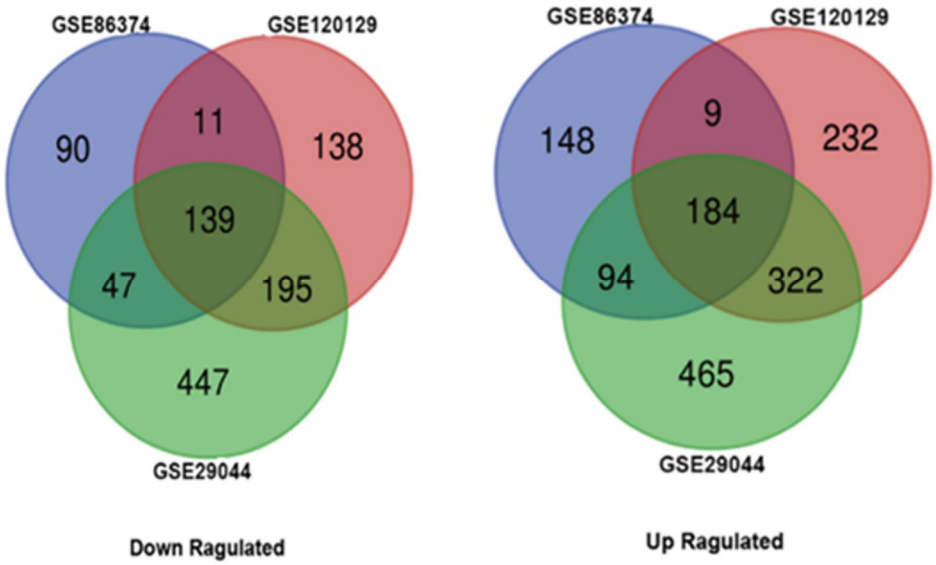

Figure 12. Down-regulated and up-regulated genes of the Venn diagram breast cancer.

Figure 13 depicts a Principal Component Analysis (PCA) to study the relationship between biological aging markers and chemotherapy treatment outcomes. The PCA figure in panel (a) distinguishes between tissue samples collected before (blue dots) and after (red triangles). The two ellipses (blue and red) indicate the data's clustering and distribution among these groupings. The first main component (Dim1), which accounts for 52.6% of the variation, appears to distinguish the pre- and post-treatment groups, implying that chemotherapy causes meaningful alterations in biological aging markers. Dim2 accounts for an extra 15.6% of the variation, which helps to further differentiate groups. The PCA figure in panel (b) is a correlation circle plot that shows how different biological aging markers influence the principal components.

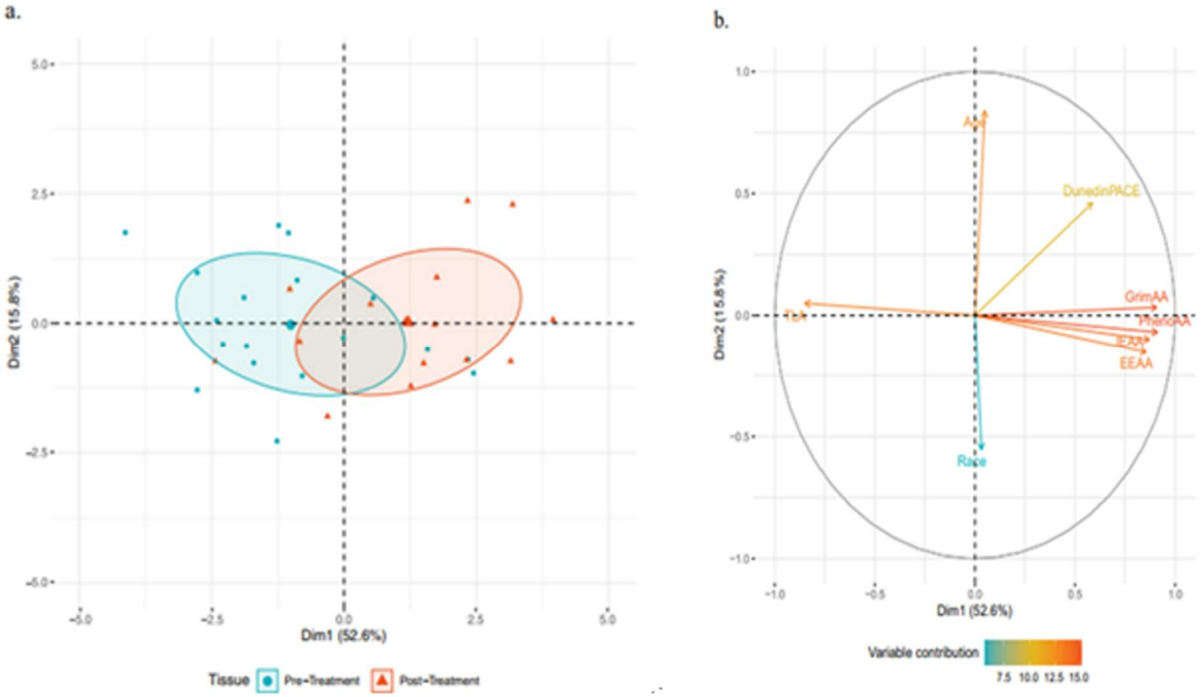

Figure 13. PCA of biological ageing markers and chemotherapy association.

Markers such as GrimAge acceleration (GrimAA), DunedinPACE, PhenoAge acceleration (PhenoAA), EEAA (Extrinsic Epigenetic Age Acceleration), and Age acceleration (AA) all have high positive relationships with Dim1, demonstrating their importance in distinguishing pre- and post-treatment states. In contrast, RACE (perhaps a resistance or alternative age-related marker) points in the opposite direction, indicating a negative relationship with the post-treatment profile. The color gradient on the vectors shows each marker's variable contribution, with orange-red indicating a stronger influence on the principal components. Overall, this data reveals that chemotherapy is associated with unique variations in biological aging profiles, as represented by several aging-related indicators.

Through the identification and targeting of particular biomarkers, biological treatments are being employed more and more to aid in early diagnosis and monitoring of breast cancer in addition to their therapeutic application. These biomarkers [29], such as HER2, estrogen and progesterone receptors, and circulating tumor DNA (ctDNA), are proteins or genetic changes linked to breast cancer that can be discovered

utilizing modern molecular imaging and diagnostic procedures. Furthermore, these biomarkers can guide individualized screening efforts, especially in high-risk people, and enable real-time monitoring of therapy response or illness recurrence. Thus, biological treatments and techniques are making breast cancer detection more precise, targeted, and patient-specific, resulting in better early diagnosis and prognosis.

The connection between computational methods and biological discoveries is crucial, since it can considerably increase the impact and interpretability of the research. While the IChOA combined with CNN-LSTM has strong classification skills, its utility can be increased by tying model-identified features to specific biological processes or biomarkers. For example, it is crucial to look into whether features discovered by the deep learning model are highly significant in the classification of breast cancer subtypes match known gene expressions, protein levels, or molecular pathways implicated in tumor progression, hormone response, or immune modulation.

By linking computationally determined attributes to biological entities, researchers can validate the model's judgments based on biological relevance, boosting the AI system's reliability. Furthermore, this relationship allows for the discovery of novel biomarkers or regulatory processes that would not be obvious using traditional analysis. Such findings can help guide future wet-lab research, stratify patient populations, and aid in the development of tailored medicines. In summary, mixing biological interpretation with computational outputs turns the model from a black-box classifier to a relevant scientific instrument that connects artificial intelligence and biomedical research.

5. Discussion

Presented an approach for identifying robust prognostic markers using biological regulatory networks in the breast cancer context. Rather than establishing signatures of genes that are differentially expressed in poor prognosis vs good prognosis samples, the method attempts to identify the upstream transcriptional regulators of the signature that are consistent with the network topology. Next A DL-based technique that effectively classifies and retrieves BreakHis pictures of the histopathology of breast cancer. Important textural and spatial features are recovered using HOG and GLCM algorithms after the images are initially cleaned using bilateral filtering on the BreakHis dataset. A CNN-LSTM network and the IChOA are combined in a potent hybrid model for classification in order to increase learning accuracy and identify intricate patterns.

Furthermore, the model had great recall and precision, both of which reached 98.18%, suggesting that it was equally successful in reducing false negatives and false positives. The model's predictions were consistent and dependable, as evidenced by the F1-score of 98.18%, which balances precision with recall. The Roc curve is displayed in **Figure 14**.

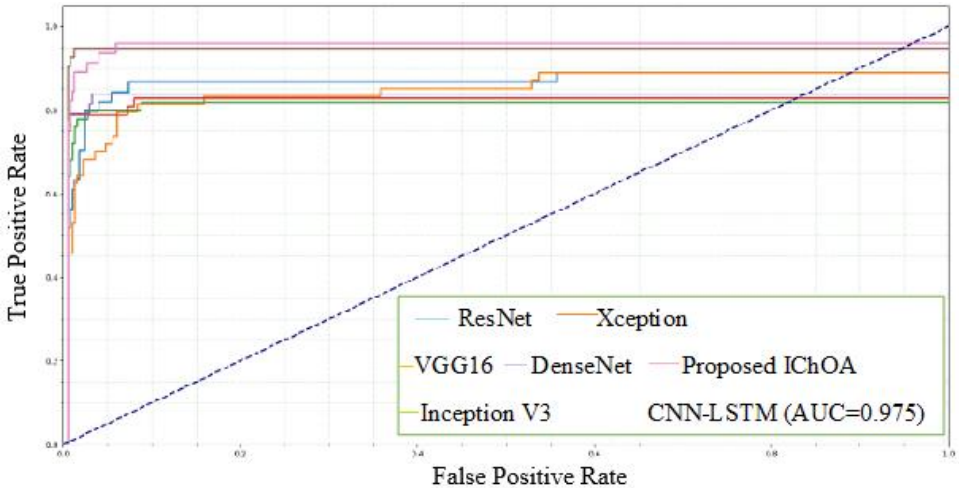

Figure 14. Suggested model is contrasted with the ROC curves of other pre-trained CNN models.

The performance of breast histopathology pictures using the suggested method and several pretrained CNN models is shown in **Table 3**. The performance analysis in relation to several models is displayed in **Figure 15**.

Table 3. Evaluation of breast histopathology images utilizing several models existing in use against the proposed approach.

Model	Accuracy	Precision	Recall	F1-Score
ResNet	88.56	88.74	88.15	88.67
VGG16	86.23	86.18	85.97	86.75
Inception V3	88.04	87.64	87.93	87.34
Xception	85.57	86.06	85.74	86.01
DenseNet	89.69	90.41	90.07	90.21
Proposed IChOA-CNN-LSTM	97.50	98.18	98.18	98.18

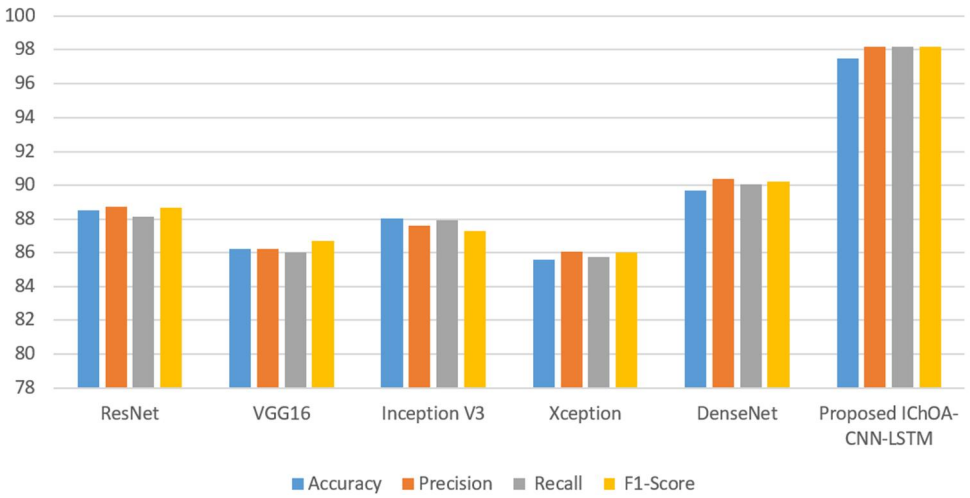

Figure 15. performance analysis compared to several models.

By giving pathologists in developing countries access to tissue images at greater magnifications, the suggested method can be a valuable tool in helping them get

around the constraints of their scanners. Through the use of greater magnifications to analyze similar patches, IChOA-CNN-LSTM CBMIR can help pathologists from various locations collaborate across borders. IChOA-CNN-LSTM CBMIR in Sen2 enables pathologists to obtain comparable instances at all four scales, in contrast to CBMIR, which only permits pathologists to obtain cases from the same magnification as their query (Q). However, storage and privacy limits make image sharing with a single server difficult. Using the suggested IChOA-CNN-LSTM CBMIR, comparable patches can be retrieved at the same or greater magnifications. The accuracy and dependability of DL models may be significantly impacted by this unpredictability. This is a significant finding because it shows that one of the main obstacles to gathering and applying WSIs in histopathology can be successfully addressed by the suggested strategy. With a more generalized, fast-trained, and accurate CBMIR, the suggested approach has addressed the concerns of both pathologists and DL scientists, according to the experimental outcomes in both scenarios and tests. **Table 4** displays the performance comparison of the proposed CBMIR model with different histopathological datasets. **Table 5** shows that the performance metrics for various strategies.

Table 4. Performance comparison of the proposed CBMIR model vs different histopathological datasets.

Dataset	Accuracy (%)	Precision (%)	Recall (%)	F1-Score (%)
BreakHis	97.5	96.8	97.2	97.0
TCGA	95.3	94.7	94.1	94.4
CAMELYON16	94.6	93.8	94.0	93.9

Table 5. Performance metrics for various strategies.

Title	Method	Accuracy (%)
Breast cancer prediction with a voting classifier method, 2017 [30]	KNN	83.45
Enhancing Breast Cancer Detection using Deep Learning [31]	CNN	88.00
Proposed	IChOA- CNN-LSTM	97.5

Limitations

Despite the high performance of the proposed CBMIR system, this study has many drawbacks. First, the model is trained and tested solely on the BreakHis dataset, which may limit its applicability to other histopathological datasets or clinical contexts with different image capture techniques. Second, the study does not include multimodal data like mammography or genetic information, which could improve diagnostic accuracy and provide a more complete clinical picture. Furthermore, the framework lacks a full investigation of computational complexity and training time, which are critical for determining its suitability in real-time clinical settings. The robustness of the model's performance may be impacted by class imbalance in the dataset, which is why no methods like data augmentation or class rebalancing are provided.

6. Conclusion

This work built a strong and intelligent biological system for categorizing and retrieving histology pictures of breast cancer. Proposed method, which makes use of the BreakHis dataset, combines sophisticated preprocessing via bilateral filtering with rich feature extraction using HOG and GLCM descriptors. Using a cascaded CNN-LSTM architecture and the Improved Chimp Optimization Algorithm (IChOA), the hybrid classification model at the heart of the system effectively learns both spatial and temporal patterns in the image data. With a 97.5% classification accuracy, the proposed framework demonstrated significant potential to support clinical diagnostic judgments. The method connects with tailored biological therapy options, including HER2-targeted antibodies and small-molecule inhibitors, by allowing for more reliable early detection of key tumor features. Integrating CBMIR into diagnostic procedures could thus serve as an effective tool for identifying and optimizing tailored therapeutic interventions, thereby boosting precision oncology and patient outcomes. The finding may hold promise for future improvements in treating BC. In order to improve feature discrimination and concentrate on tissue regions that are diagnostically significant, future studies can investigate the incorporation of attention mechanisms into the IChOA-CNN-LSTM structure. The system's diagnostic insights could also be further enhanced by the addition of multi-modal data, such as genetic markers or clinical records.

Author contributions: Conceptualization, SDC and AKC; methodology, SDC; software, SDC; validation, SDC and AKC; formal analysis, AKC; investigation, SDC; resources, AKC; data curation, SDC; writing—original draft preparation, SDC; writing—review and editing, AKC; visualization, SDC; supervision, AKC; project administration, SDC; funding acquisition, AKC. All authors have read and agreed to the published version of the manuscript.

Acknowledgments: I want to express my gratitude to my respected supervisor and the head of the department for their leadership.

Institutional review board statement: Not applicable.

Informed consent statement: Not applicable.

Availability of data and material: Upon reasonable request, the accompanying author is able to supply the data that supports the findings of the investigation.

Conflict of interest: The authors declare no conflict of interest.

References

1. Shetty R, Bhat VS, Pujari J. Content-based medical image retrieval using deep learning-based features and hybrid meta-heuristic optimization. Biomedical Signal Processing and Control. 2024; 92: 106069. doi: 10.1016/j.bspc.2024.106069
2. Silva-Gomes R, Caldeira I, Fernandes R, et al. Metabolic regulation of the host–fungus interaction: from biological principles to therapeutic opportunities. Journal of Leukocyte Biology. 2024; 116(3): 469-486. doi: 10.1093/jleuko/qiae045
3. din ud NM, Dar RA, Rasool M, et al. Breast cancer detection using deep learning: Datasets, methods, and challenges ahead. Computers in Biology and Medicine. 2022; 149: 106073. doi: 10.1016/j.compbiomed.2022.106073
4. Kaur J, Kaur P. A systematic literature analysis of multi-organ cancer diagnosis using deep learning techniques. Computers in Biology and Medicine. 2024; 179: 108910. doi: 10.1016/j.compbiomed.2024.108910

5. Gou F, Liu J, Xiao C, et al. Research on Artificial-Intelligence-Assisted Medicine: A Survey on Medical Artificial Intelligence. Diagnostics. 2024; 14(14): 1472. doi: 10.3390/diagnostics14141472
6. Harshvardhan GM, Sahu A, Gourisaria MK, et al. On the Dynamics and Feasibility of Transferred Inference for Diagnosis of Invasive Ductal Carcinoma: A Perspective. IEEE Access. 2022; 10: 30870-30889. doi: 10.1109/access.2022.3159700
7. Ghosh T, Jayanthi N. Impact of preprocessing techniques on MRI-based brain tumor detection. Multimedia Tools and Applications; 2025. doi: 10.1007/s11042-025-20633-4
8. Khan S, Islam N, Jan Z, et al. A novel deep learning based framework for the detection and classification of breast cancer using transfer learning. Pattern Recognition Letters. 2019; 125: 1-6. doi: 10.1016/j.patrec.2019.03.022
9. Hirra I, Ahmad M, Hussain A, et al. Breast Cancer Classification From Histopathological Images Using Patch-Based Deep Learning Modeling. IEEE Access. 2021; 9: 24273-24287. doi: 10.1109/access.2021.3056516
10. Gour M, Jain S, Sunil Kumar T. Residual learning based CNN for breast cancer histopathological image classification. International Journal of Imaging Systems and Technology. 2020; 30(3): 621-635. doi: 10.1002/ima.22403
11. Fang Y, Zhao J, Hu L, et al. Image classification toward breast cancer using deeply-learned quality features. Journal of Visual Communication and Image Representation. 2019; 64: 102609. doi: 10.1016/j.jvcir.2019.102609
12. Liu M, Hu L, Tang Y, et al. A Deep Learning Method for Breast Cancer Classification in the Pathology Images. IEEE Journal of Biomedical and Health Informatics. 2022; 26(10): 5025-5032. doi: 10.1109/jbhi.2022.3187765
13. Jo YY, Choi YS, Park HW, et al. Impact of image compression on deep learning-based mammogram classification. Scientific Reports. 2021; 11(1). doi: 10.1038/s41598-021-86726-w
14. Nasser M, Yusof UK. Deep Learning Based Methods for Breast Cancer Diagnosis: A Systematic Review and Future Direction. Diagnostics. 2023; 13(1): 161. doi: 10.3390/diagnostics13010161
15. Mehta AK, Kadel S, Townsend MG, et al. Macrophage Biology and Mechanisms of Immune Suppression in Breast Cancer. Frontiers in Immunology. 2021; 12. doi: 10.3389/fimmu.2021.643771
16. Zakareya S, Izadkhah H, Karimpour J. A New Deep-Learning-Based Model for Breast Cancer Diagnosis from Medical Images. Diagnostics. 2023; 13(11): 1944. doi: 10.3390/diagnostics13111944
17. Yari Y, Nguyen TV, Nguyen HT. Deep Learning Applied for Histological Diagnosis of Breast Cancer. IEEE Access. 2020; 8: 162432-162448. doi: 10.1109/access.2020.3021557
18. Sahu A, Das PK, Meher S. Recent advancements in machine learning and deep learning-based breast cancer detection using mammograms. Physica Medica. 2023; 114: 103138. doi: 10.1016/j.ejmp.2023.103138
19. Sharma A, Mishra PK. Performance analysis of machine learning based optimized feature selection approaches for breast cancer diagnosis. International Journal of Information Technology. 2021; 14(4): 1949-1960. doi: 10.1007/s41870-021-00671-5
20. Arya N, Saha S. Multi-Modal Classification for Human Breast Cancer Prognosis Prediction: Proposal of Deep-Learning Based Stacked Ensemble Model. IEEE/ACM Transactions on Computational Biology and Bioinformatics. 2022; 19(2): 1032-1041. doi: 10.1109/tcbb.2020.3018467
21. Narayanan L, Krishnan S, Robinson H. A Hybrid Deep Learning Based Assist System for Detection and Classification of Breast Cancer from Mammogram Images. The International Arab Journal of Information Technology. 2022; 19(6). doi: 10.34028/iajit/19/6/15
22. Kavitha T, Mathai PP, Karthikeyan C, et al. Deep Learning Based Capsule Neural Network Model for Breast Cancer Diagnosis Using Mammogram Images. Interdisciplinary Sciences: Computational Life Sciences. 2021; 14(1): 113-129. doi: 10.1007/s12539-021-00467-y
23. Gupta S, Agrawal S, Singh SK, Kumar S. A novel transfer learning-based model for ultrasound breast cancer image classification. In: Computational Vision and Bio-Inspired Computing: Proceedings of ICCVBIC 2022. Singapore: Springer Nature Singapore; 2023.
24. Xiao M, Zhao C, Zhu Q, et al. An investigation of the classification accuracy of a deep learning framework-based computer-aided diagnosis system in different pathological types of breast lesions. Journal of Thoracic Disease. 2019; 11(12): 5023-5031. doi: 10.21037/jtd.2019.12.10
25. Alnbaheen MS, Ikbal AMA, Bekhit MMS, et al. Exploring Interplay of Polyunsaturated Fatty Acids: A Promising Approach for Treatment of Breast Cancer. Journal of biological regulators and homeostatic agents. 2024. doi: 10.23812/j.biol.regul.homeost.agents.20243809.463

26. Garban Z, Ilia G. Structure-Activity of Plant Growth Bioregulators and Their Effects on Mammals. Molecules. 2024; 29(23): 5671. doi: 10.3390/molecules29235671
27. Ovchinnikov AYu, Miroshnichenko NA, Nikolaeva YuO. Possibilities of bioregulation therapy in the treatment of patients with chronic tonsillitis. Farmakoekonomika Modern Pharmacoeconomics and Pharmacoepidemiology. 2023; 16(4): 587-595. doi: 10.17749/2070-4909/farmakoekonomika.2023.224
28. Kalupahana NS, Moustaid-Moussa N. Beyond blood pressure, fluid and electrolyte homeostasis—Role of the renin angiotensin aldosterone system in the interplay between metabolic diseases and breast cancer. Acta Physiologica. 2024; 240(7). doi: 10.1111/apha.14164
29. Chen Y, Sun Y, Cai W, et al. TFDP1 Enhances the Malignant Biological Behaviors of Breast Cancer Cells by Promoting ASF1B-mediated CKS1B Upregulation. Journal of biological regulators and homeostatic agents. 2024; 38(4). doi: 10.23812/j.biol.regul.homeost.agents.20243804.255
30. Kumar UK, Nikhil MBS, Sumangali K. Prediction of breast cancer using voting classifier technique. In: Proceedings of the 2017 IEEE International Conference on Smart Technologies and Management for Computing, Communication, Controls, Energy and Materials (ICSTM); 2017. doi: 10.1109/icstm.2017.8089135
31. Shen L, Margolies LR, Rothstein JH, et al. Deep Learning to Improve Breast Cancer Detection on Screening Mammography. Scientific Reports. 2019; 9(1). doi: 10.1038/s41598-019-48995-4